THE ASTROPHYSICAL JOURNAL, 473:483–493, 1996 December 10

AR URSAE MAJORIS: THE FIRST HIGH-FIELD MAGNETIC CATACLYSMIC VARIABLE

GARY D. SCHMIDT,[1] PAULA SZKODY,[2] PAUL S. SMITH,[1,3] ANDREW SILBER,[2] GAGHIK TOVMASSIAN,[4]
D. W. HOARD,[2] B. T. GÄNSICKE,[5] AND D. DE MARTINO[6]

Received 1996 June 3; accepted 1996 July 8

ABSTRACT

We identify the luminous soft X-ray source AR UMa as a magnetic cataclysmic variable containing a white dwarf with the highest field yet detected in an accreting binary. *IUE* and optical spectroscopy, optical photometry, and circular polarimetry and spectropolarimetry define remarkably distinct accretion states of this binary. Circular polarization is nearly absent in the high state, but the low state exhibits values which vary between 2% and 5% on the orbital period of 1.932 hr. The UV continuum contains a broad absorption feature near 1300 Å, while optical spectropolarimetry during the low state reveals a number of strongly polarized dips. These are interpreted as Zeeman components of hydrogen Lyα and another atmospheric species, possibly He I, in a photospheric magnetic field of $\sim$230 MG.

The radial velocity curve of the low-state optical emission lines shares the period of the optical photometry and polarimetry and is phased appropriately for an origin on the irradiated secondary star. While the high state exhibits prominent UV line emission typical of the magnetic variables, the strength of the UV continuum does not vary appreciably with a change in accretion state. This, combined with the high soft X-ray luminosity and lack of circular polarization, indicates that accretion occurs largely in the form of dense filaments which avoid a standoff shock and thermalize their kinetic energy below the white dwarf photosphere. We suggest that these phenomena may play a role in the apparent lack of high-field systems with easily detectable circular polarization during high-accretion states.

Subject heading: binaries: spectroscopic — novae, cataclysmic variables — stars: individual (AR UMa) — stars: magnetic fields — ultraviolet: stars

1. INTRODUCTION

The cataclysmic variable AR UMa was identified as the optical counterpart of a highly variable X-ray source (1ES 1113+432) in the *Einstein* Slew Survey by Remillard et al. (1994; hereafter RS[3]). Two IPC observations in 1979 November and 1980 May showed count rates that varied from 2 to 43 counts s^{-1}, with analysis of the brighter state showing a very soft spectrum ($\sim$22 eV blackbody). A search through the Harvard Plate Library documented high states near $B = 13.5$–14.0 and low states down to 16th magnitude. Optical spectroscopy during a low state in 1991 June revealed an M6 dwarf with narrow Balmer emission lines, implying a distance of $\sim$88 pc. *I*-band photometry during low states in 1992 June and 1993 May showed quasi-sinusoidal variations which were interpreted as ellipsoidal variations in the M star with a binary period of 1.932 hr. With the inferred distance, the blackbody X-ray luminosity was estimated to be 3×10^{33} ergs s^{-1}, one of the largest values yet derived for a CV (e.g., Norton & Watson 1989) and especially so for one at a short orbital period.

The above properties led RS[3] to suggest that AR UMa was a member of the AM Her class of cataclysmic variables. In these systems, a white dwarf magnetic field in the range $\sim$10–70 MG (MG = 10^6 G) dominates the accretion flow near the primary star and prevents the formation of an accretion disk (e.g., Cropper 1990). Synchronization of the spin of the white dwarf to the binary motion also results from a strong magnetic interaction between the two stars. While the disk-dominated, asynchronous DQ Her variables (so-called intermediate polars) apparently represent magnetic fields weaker than the above range, the lack of very strongly magnetic (greater than 100 MG) primaries among known CVs is a mystery since such high values have been found among white dwarfs in the field.

Classification of AR UMa as an AM Her–type binary hinges upon obtaining a detection of circular polarization from cyclotron emission radiated at the accretion shock, the hallmark of all such objects. The Roboscope light curves (Honeycutt, Robertson, & Turner 1996) reveal that the object was in a high state for most of 1995 except for a brief low during February and March. In November it entered a low state and remained there through at least 1996 March. This paper reports *IUE* and optical spectroscopy, optical photometry, and circular polarimetry and spectropolarimetry during both accretion states which reveal AR UMa to be a remarkable new member of the class of magnetic variables and the first example of the long-sought systems with $B > 100$ MG.

The next section briefly describes the observations. Section 3 presents evidence for a high magnetic field strength on the primary star. Subsequent sections discuss the observed characteristics of AR UMa in terms of the accretion physics, emission components, and evolution of a high-field system. We conclude with a brief summary.

2. OBSERVATIONS

On 1995 April 12, a 35 minute short-wavelength, low-resolution spectrum in the large aperture (SWP 54401) was

[1] Steward Observatory, University of Arizona, Tucson, AZ 85721; gschmidt@as.arizona.edu.
[2] Astronomy Department, University of Washington, Seattle, WA 98195; szkody@astro.washington.edu, silber@astro.washington.edu, hoard@astro.washington.edu.
[3] Current address: National Optical Astronomy Observatories, Kitt Peak National Observatory, P.O. Box 26732, Tucson, AZ 85726-6732; psmith@noao.edu.
[4] Instituto de Astronomía-UNAM, Apdo Postal 877, 22860, Ensenada, B.C., Mexico; gag@bufadora.astrosen.unam.mx.
[5] Universität-Sternwarte, Geismarlandstrasse 11, D-37083, Göttingen, Germany; boris@uni-sw.gwdg.de.
[6] Osservatorio Astronomico di Capodimonte, via Moiariello 16, 80131 Napoli, Italy; demartino@astrna.na.astro.it.

TABLE 1

CHRONOLOGY OF OBSERVATIONS

Date	UT	State (V)	Telescope	Instrument	Exposure[a]	Filter/λ (Å)
1995 Apr 12	16:30	High	*IUE*	SWP	35	1175–2000
1995 Apr 12	3:30	High (~14.5)	APO 3.5 m	DIS Spec	5	4300–6800
1995 Apr 6.....	4:54–8:34	High	OAN 1.5 m	CCD Imager	2	*B*
1995 Apr 30	7:21–8:24	High	OAN 1.5 m	CCD Imager	1	*B*
1995 May 1.....	4:15–6:23	High	OAN 1.5 m	CCD Imager	1	*B*
1995 May 5.....	4:06–6:29	High (~15)	OAN 1.5 m	CCD Imager	1	*V*
1995 Oct 24	11:50–12:23	High	SO 1.5 m	TwoHoler Pol	4	3200–8600
1995 Oct 25	12:10–12:25	High (~15.3)	SO 1.5 m	TwoHoler Pol	4	3200–8600
1995 Nov 19.....	11:31–12:16	Low	SO 1.5 m	TwoHoler Pol	5	3200–8600
1995 Nov 20.....	12:11–12:18	Low	SO 1.5 m	TwoHoler Pol	7	3200–8600
1995 Nov 21.....	12:13–12:28	Low (16.6)	SO 2.3 m	Spectropol	8	4650–7150
1995 Nov 23.....	12:16–12:28	Low (16.5)	SO 2.3 m	Spectropol	12	4650–7150
1995 Dec 15	10:20	Low	*IUE*	SWP	116	1175–2000
1996 Jan 14.....	8:45–11:17	Low (16.6)	SO 2.3 m	B&C Spec	8	4000–5200
1996 Jan 27.....	5:22–7:18	Low (16.6)	SO 2.3 m	Octopol	2	3200–8600
1996 Feb 18	8:30–11:55	Low	OAN 1.5 m	CCD Imager	3	*I*
1996 Mar 16.....	6:48–8:51	Low (16.8)	SO 2.3 m	Spectropol	10	4340–7450

[a] Sample time in minutes for time series.

obtained with the *International Ultraviolet Explorer* satellite. On the same day, an optical spectrum was obtained with the 3.5 m telescope at Apache Point Observatory using the double imaging spectrograph in high-resolution mode (2 Å). Although standard stars were observed, the lack of a guider or slit viewer prevented any certainty about the absolute flux level, so only relative fluxes are reliable. A broadband CCD image (3900–5300 Å) obtained with the spectrograph in imaging mode established a crude magnitude of about $V \sim 14.5$ by comparison with stars of known magnitude.

Between 1995 April 6 and May 5, three nights of photometry were obtained in B and one night in the V filter using a CCD on the 1.5 m telescope of the Observatorio Astronomico Nacional de San Pedro Martir. Because of the sparseness of the surrounding field, differential photometry with respect to a comparison star on the same frame was only accomplished on the last night. On April 30 and May 1, a comparison star was measured on separate frames every half-hour, and a linear interpolation was used to obtain a differential light curve. The data from April 6 are in instrumental magnitudes, while the rest of the nights have an approximate calibration from comparison to Landolt standards obtained the same night. An additional 3.5 hr of I-band data obtained with the same instrument and telescope in 1996 February provided information on the low state. Because of the different sensitivity and noise characteristics at blue and red wavelengths, the error bars on the B measurements may be as large as 0.2 mag while those for the I band are ~0.03 mag.

Optical polarimetry of AR UMa was obtained at Steward Observatory on several occasions between 1995 October 24 and 1996 March 16, using a variety of telescopes and instruments. Only two measurements (1995 October 24 and 25) were accomplished before the system entered a low state, but observations after that point include time series measurements covering complete orbital cycles.

A full cycle of optical spectrophotometry allowed measurement of the radial velocity and brightness modulation of the emission lines during the low state. These were obtained with the Steward Observatory 2.3 m telescope and facility spectrograph operating over the spectral region Hδ–Hβ at a resolution of 2 Å (~110 km s^{-1}).

Finally, a low-state spectrum with *IUE* was added on 1995 December 15 (SWP 56296). This 115.8 minute exposure differs dramatically from the high-state spectrum, with all prominent high-state emission lines having disappeared.

All observations are summarized in Table 1. From left to right, the columns list the UT date and time, the accretion state (and estimate of V-band magnitude, if available), the observing facility and instrument, the exposure time, and

TABLE 2

HIGH-STATE UV LINE MEASUREMENTS

Line	Flux (10^{-13} ergs cm^{-2} s^{-1})	EW (Å)
N v λ1239+43	7.9	39
Si iii λ1300.....	0.9	5
C ii λ1334.....	2.1	11
Si iv λ1393+1402.....	6.2	26
C iv λ1548+50.....	26.1	152
He ii λ1640	6.3	45

TABLE 3

OPTICAL LINE MEASUREMENTS IN HIGH AND LOW STATES[a]

Line	High-State EW	High-State Flux	Low-State EW	Low-State Flux
Hδ	...	...	2	6
Hγ.....	46	130	3	7
He i λ4471	17	48	...	...
He ii λ4686.....	52	130	0.5	1
Hβ	67	140	7	10
He i λ4922	12	25	1.2	1.6
He i λ5015	11	23	1.8	2.3
Fe ii λ5169	...	...	2	2.6
Fe ii λ5272	...	...	1.2	1.3
He i λ5876	23	31	5	4
Hα	121	130	41	26
He i λ6678	22	23	3	1.8

[a] EW is in units of Å; flux is in units of 10^{-15} ergs cm^{-2} s^{-1}. Due to large light losses at the slit, only flux ratios are reliable for the high-state data. Line fluxes vary around the orbit and with epoch, even during a given activity state. Values shown are representative.

the wavelength region studied. The emission-line fluxes and equivalent widths as measured from the high- and low-state spectra are contained in Tables 2 and 3.

3. A HIGHLY MAGNETIC WHITE DWARF

3.1. *Broadband Behavior*

Lacking the storage provided by an accretion disk, the AM Her–type magnetic CVs are prone to large fluctuations in brightness with variations in mass transfer through the L1 point. From available photometry, AR UMa appears to be unusually bimodal even for the synchronized systems. The circular polarization measured on consecutive nights in 1995 October (with $V \sim 15.3$, when the system was moderately active) was remarkably small, $V/I = +0.33\% \pm 0.08\%$ and $+0.52\% \pm 0.18\%$, respectively, despite time series which lasted up to 30% of the orbital cycle. Although the polarity of these results is the same as that found in ensuing measurements, the polarization is much weaker than at any time during the low-state cycle and weaker than the phase-averaged optical polarization of any other active AM Her system.

As shown by the broadband time series in Figure 1 and Table 1, the low state entered in late 1995 was characterized by $V \sim 16.6$ and circular polarization varying sinusoidally between $+2.2\%$ and $+4.3\%$ on the 1.9 hr period. Hence, AR UMa must be regarded as at least approximately synchronized and a bona fide magnetic system. The peak polarization, as derived from the least-squares fit shown in the figure, occurred on HJD $2{,}450{,}109.8129 \pm 0.0023$. Notably, the broadband count rate in this low-accretion state was constant to within 10% of the mean brightness on both epochs with full orbital coverage (1996 January 27 and 1996 March 16).

A uniform sign of circular polarization during the entire rotational cycle indicates an orientation in which one magnetic pole is continuously in view. For a centered dipole, this implies that the sum of the inclination and magnetic pole colatitude $i + \delta < \pi/2$. While more extensive measurements are required in a high state, the anticorrelation between accretion state and degree of polarization further suggests that, if cyclotron emission is a significant contributor to the high-state light, it must be optically thick. In the canonical interpretation, this implies (1) an unusually strong magnetic field on the primary (such that the cyclotron fundamental lies near the optical), and/or (2) an unusually high accretion rate.

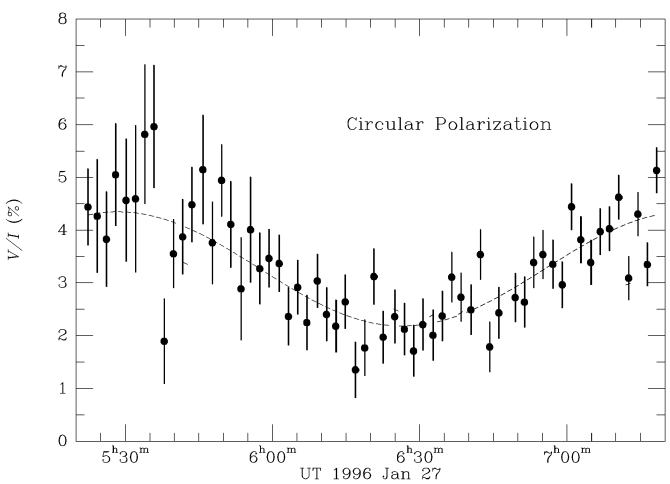

FIG. 1.—Variation of broadband circular polarizationimately one orbital cycle during the low state in 1996 January. The dashed curve is a best-fit sinusoid of period equal to the 1.932 hr photometric value.

3.2. *The Optical Zeeman Spectrum*

In a number of AM Her systems the strength of the magnetic field on the primary star has been measured through photospheric Zeeman absorption and circular polarization features in low-state spectra (e.g., Schmidt, Stockman, & Margon 1981; Wickramasinghe, Visvanathan, & Tuohy 1984; Schwope et al. 1993). The pattern seen is a mean over the observable hemisphere, weighted by the surface brightness. Thus far, all spectral features have been attributable to hydrogen, and field strengths span the rather restricted range $B_p \sim 7$–70 MG (Ferrario et al. 1994; Schwope et al. 1995).

The low-state spectra from all sources are presented in Figure 2 together with the spectrum of circular polarization co-added over the 1996 March sequence with the spectropolarimeter. The flux spectra display strong band heads from the M6 companion in the red plus a rising continuum shortward of $\sim$6000 Å which is checkered with numerous weak absorption features. Notable among the latter are a sharp blue-edged trough centered near λ5920, a pair of somewhat narrower features straddling λ5500, and two very broad dips near λ4500 and λ4650. As summarized in Table 4, these and other weaker lines are accompanied by positive and negative circular polarization features as large as $\Delta(V/I) \sim 5\%$. Although there are subtle changes in the locations and shapes of the features phased with the rotational cycle, the basic character of the spectrum persists through-

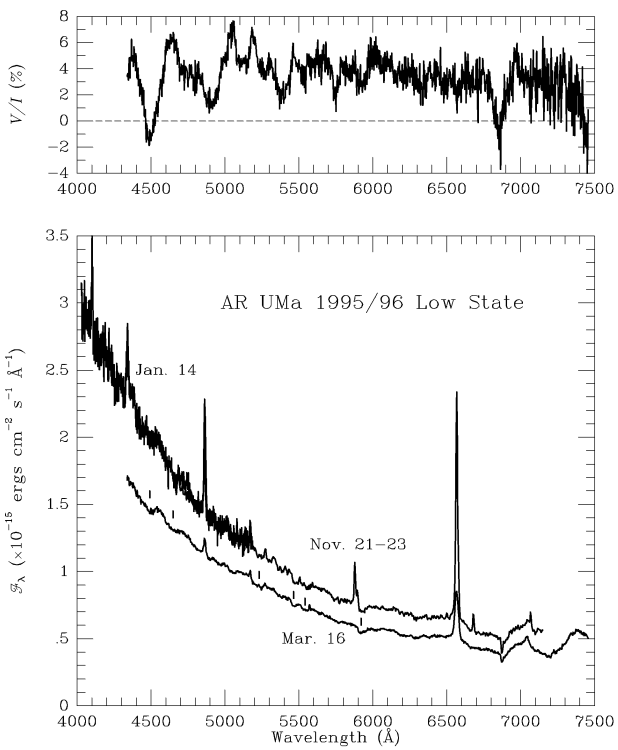

FIG. 2.—*Bottom*: comparison of optical spectra obtained during the 1995–1996 low state. *Top*: net circular polarization spectrum co-added over a full rotational cycle in 1996 March. Note the existence of a number of unidentified, strongly polarized absorption features (marked in the total flux spectrum).

TABLE 4

UNIDENTIFIED OPTICAL ABSORPTION LINES IN THE LOW STATE

Feature	Wavelength (Å)	Circular Polarization[a]
a	4485	...
b	4630	+
c	4800	u
d	4890	...
e	4960	u
f.....	5045	+
g	5200	+
h	5375	...
i.....	5460	u
j.....	5545	u
k	5760	...
l.....	5915	...
m	6850	...

[a] Sign of circular polarization. The letter "u" indicates a feature which appears to be unpolarized.

out. The irregular spacing and rough spectral appearance are in stark contrast to the smoothly undulating cyclotron emission harmonics often present in the spectra of AM Her systems when actively accreting. The features better resemble photospheric Zeeman lines from a strongly magnetic white dwarf. Indeed, when the strength of the polarization feature at 4500 Å is coupled with the constancy of the low-state brightness, the inference is that the white dwarf must be responsible for most, if not all, of the light below ~5500 Å, i.e., accretion may have abated altogether. Among isolated white dwarfs, disk-averaged continuum polarization of $|V/I| \gtrsim 5\%$ has only been seen in stars with $B \gtrsim 200$ MG (Schmidt, Latter, & Foltz 1990).

Now that transition wavelengths and strengths are available for the important lines of hydrogen over a very wide range in B (e.g., Ruder et al. 1994), the process of modeling a photospheric spectrum like that in Figure 2 can provide a detailed picture of the field strength and morphology over the surface of a magnetic white dwarf. Above ~100 MG, however, uncertainties arise as a result of (unknown) magnetic effects on the continuum opacities and structure of the stellar atmosphere. In this domain, techniques which ignore radiative transfer and treat the flux spectrum alone are not markedly inferior to more elaborate approaches, and they still yield accurate diagnoses of the field strengths present. Using such a simplified code (Latter, Schmidt, & Green 1987), we have made a thorough comparison of the low-state spectrum of AR UMa to synthetic spectra of hydrogen over the range 0–1500 MG. The observed spectrum is complex and a number of the Balmer transitions are rapidly moving, so some matches can always be found. However, for a realistic field pattern with a range in B over the stellar surface, the most prominent features are those which are near stationary or turnaround points in their behavior. In situations where these approximate observed features in AR UMa, other lines which would be expected are missing and/or additional features which are present in the data go unexplained. We conclude that the optical spectrum of AR UMa must be wholly or in part due to an atmospheric species other than hydrogen. In this respect, the star resembles the two isolated white dwarfs the spectra of which are still a mystery: GD 229 (Schmidt et al. 1996) and LB11146b (Liebert et al. 1993; Glenn, Liebert, & Schmidt 1994). (Note, however, that AR UMa fails to match in detail the spectra of either of these stars.)

Unfortunately, hydrogen is the only species with a magnetic spectrum that is well understood. An alternate possibility is that all or part of the spectrum is due to neutral helium. The behavior of a number of common He I transitions was calculated by Kemic (1974) using perturbation techniques, an approach which is valid up to ~20 MG. The array of features observed in AR UMa bears no resemblance to the simple patterns expected in this regime. Recently, significant progress has been reported in solving the general three-body problem in strong magnetic fields. Thurner et al. (1993; see also Ruder et al. 1994) present energy levels, wavelengths, and transition probabilities for several two-electron atoms using both high- and low-field configurations. Unfortunately, the number of transitions studied is very limited, and the correspondence between the two computational approaches is rather poor in the intermediate regime (appropriate for magnetic white dwarfs). Thus, while it is tempting to draw correspondences between some of the features in Table 4 and lines in the predicted spectrum, calculations to date are neither sufficiently accurate nor extensive to test against the complicated spectrum which is observed.

3.3. *Clues from the Ultraviolet*

We have argued that the low-state continuum in the visible is dominated by the white dwarf. Though our high-state *IUE* spectrum is of poorer statistical quality as a result of a shorter exposure time, the 1200–2000 Å continuum in this state (Fig. 3, *top*) is no brighter than in the low state (Fig. 3, *bottom*). This is true despite the complete disappearance of the prominent emission-line component and provides a strong argument against cyclotron and/or

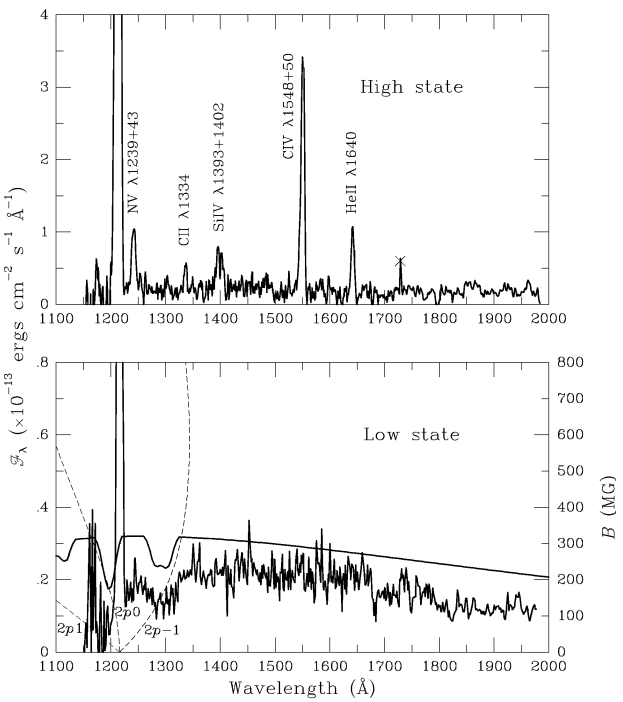

FIG. 3.—Comparison of *IUE* spectra of AR UMa obtained in high- and low-accretion states (*top* and *bottom*, respectively) . Also shown in the bottom panel is a synthetic spectrum for hydrogen for a dipole field of strength $B_p = 230$ MG. The $2p - 1$ to $1s0$ component of Lyα is approaching its red turnaround, which occurs at 1341 Å for $B = 470$ MG.

thermal emission from the accretion region being a significant part of the observed UV continuum in either state. Instead, the white dwarf photosphere likely dominates, a conclusion which we show in § 4.3 to be supported by fits to the combined UV/optical low-state continuum energy distribution.

With this interpretation, one feature in the low-state UV spectrum is of considerable significance: the broad absorption line of ~30% depth situated ~100 Å longward of geocoronal Lyα. The feature is too broad to be the Si III line often seen in the spectra of CVs and falls well short of the location of the quasi-molecular H_2 absorption which appears near 1400 Å in some DA white dwarfs. The spectrum of AR UMa better resembles the isolated white dwarf PG 1031+234 (Schmidt et al. 1986b), where a deep feature centered at ~1350 Å was attributed to the the $1s0$ to $2p-1$ component of Lyα in a magnetic field of ~500 MG. An array of optical features of hydrogen confirmed that identification. Lyα is a simple Zeeman triplet at all field strengths. Only the $1s0$ to $2p-1$ component is split longward of the zero-field location, reaching a wavelength maximum at $\lambda = 1341$ Å for $B = 470$ MG before slowly turning to the blue at higher fields. Assignment of the ~1300 Å feature in AR UMa to this component therefore suggests one of two field strength regimes: either $B \sim 200$ MG or $B = 1000$–2000 MG.

Using the computer code and transition grids described in § 3.2, the best fit to the UV observed spectrum is obtained for the lower field value. The model shown by the smooth solid line in Figure 3 corresponds to a centered dipole with $B_p = 230$ MG oriented at 30° to the line of sight, here superposed on a blackbody continuum of $T = 23{,}000$ K. The synthetic spectrum provides a good match to the location and width of the observed absorption feature, and the $2p0$ to $1s0$ (π) component may combine with the reseau near λ1197 to produce the apparent flux deficit below the geocoronal emission line. By comparison, the high-field option yields a synthetic line which is both too narrow and very asymmetric in appearance. The π line has also shifted well out of the observable UV in fields this strong.

There is a suggestion of an additional red-shaded absorption edge at ~1675 Å. Although a number of the optical transitions of H shift into the UV in high magnetic fields, we have been unable to find a consistent interpretation for both this and the λ1300 feature in terms of hydrogen and therefore attribute the λ1675 edge to a second atmospheric constituent. Note that a precedent exists for the curious situation in which an unknown species dominates the optical but Lyα appears in the UV: the strongly magnetic "*b*" member of the double-degenerate white dwarf binary LB 11146 (Liebert et al. 1993).

The emission lines of C IV, He II, N V, and Si IV which are prominent in the high-state UV spectrum of AR UMa are typical of magnetic variables (Bonnet-Bidaud & Mouchet 1987; de Martino 1995). The observed continuum shape, $F_\lambda \propto \lambda^{-1.5}$, suggests a 1200–3100 Å luminosity of 4×10^{31} ergs s^{-1} (for $d = 88$ pc). The total line luminosity (Table 2) is 0.5×10^{31} ergs s^{-1}, implying a line-to-continuum luminosity ratio which is high but not off the scale for AM Her in general (de Martino 1995).

It is useful to note that the Rayleigh-Jeans tail of the 22 eV blackbody proposed by RS[3] actually overpredicts the observed brightness of the UV continuum. Since the continuum is not observed to decline with a change in accretion state, it would appear that the temperature of the soft X-ray component must have been underestimated.

4. NATURE OF THE BINARY SYSTEM

4.1. *Geometry*

AR UMa is the first high-field ($B_p > 100$ MG) example of a synchronized magnetic CV. In low states (which are more the rule than the exception in this object), the light is primarily stellar in origin: Zeeman-split absorption features from the white dwarf for $\lambda \lesssim 6000$ Å and the photosphere of an M-type companion in the red. The visible-light circular polarization of 2%–5% in the low state is consistent with that of a naked (nonaccreting) white dwarf with a 230 MG field rotating in synchronism with the 1.9 hr orbital period.[7]

The orbital motions and emission components are best inferred from the high-resolution spectroscopy and photometry presented in § 4.3. However, our optical spectropolarimetry during the March 7 low state provides *simultaneous* information on the circular polarization, brightness of the red continuum, and emission-line radial velocities over a full orbital cycle. While there is no substitute for long-term monitoring in establishing the synchronism of a system, the spectropolarimetry are ideal for identifying the phase relationships which existed at that particular epoch. It is clear from these data that the velocity extrema coincide with maxima in the ellipsoidal brightness variations, confirming that the dominant source of emission lines in the low state is the inner Roche surface of the secondary star. The fact that the peaks in circular polarization are also phased precisely with the velocity peaks ($\Delta\phi < 0.03$) further indicates that the the field pattern is oriented at *right angles* to the stellar line of centers. This conclusion holds regardless of whether we view a cyclotron funnel or magnetized photosphere during the low state.

For comparison, previously studied AM Her systems show a strong tendency for the pole to lead the secondary by $\langle\psi\rangle \sim 20°$ (Liebert & Stockman 1985; Cropper 1988). Ideas explored in an effort to explain this clustering include the intrinsic dipole-dipole interaction in the presence of an accretion torque (Campbell 1989; King, Whitehurst, & Frank 1990), offset-dipole and quadrupolar geometries (Wickramasinghe & Wu 1991; Wu & Wickramasinghe 1993), and gravitational torques (Katz 1989; Campbell 1990). The only mechanism which explicitly predicts an equilibrium configuration in which the white dwarf field is orthogonal to the binary ($\psi = 90°$) is the dipole-induced dipole model of Joss, Katz, & Rappaport (1979). Generally accepted to be too weak to counter the accretion torque in a typical AM Her with $B \sim 30$ MG, the interaction scales as the square of the primary's magnetic moment $\mu = BR^3 \sim 2 \times 10^{35}$ G cm^3 for $B \sim 200$ MG. If convection within the secondary leads to increased dissipation (Campbell 1983), the mechanism is further enhanced. Of course, the effect is greatest when the stars are detached. At a period of 1.93 hr, it is conceivable that AR UMa has just emerged from the period gap and thus temporarily retains that orientation (however, see § 6 below). It is important in this context to remember that the mechanisms for *achieving* synchronism and for *maintaining* it may differ (e.g., Lamb 1985; Lamb & Melia 1988).

[7] In fields this strong, we would also expect significant linear polarization in the continuum and certain Zeeman lines, varying on the spin period.

4.2. *Emission Components in the High State*

Not only does the cyclotron fundamental fall in the optical window ($\lambda_c = 4660$ Å for $B_p = 230$ MG), the more or less pole-on orientation increases the cyclotron opacity in our direction. Both tend to reduce the polarized emission when the system is actively accreting. The fact that the stream is continuously in view also maximizes the amount of reprocessed light from the funnel. It is interesting to note that our high-state polarization of $V/I \sim +0.4\%$ is consistent with simple dilution of the low-state polarized flux for the observed brightness increase of 2–3 mag. Hence, the added accretion light may be unpolarized altogether.

Typically, the optical emission of AM Her stars during high states is dominated by components originating in the accretion stream and column. For AR UMa, high-state data of any type are sorely lacking; however, what is available supports this origin. Figures 4*a*–4*c* present high-state light curves from the period 1995 April–May. Though flickering appears to play an important role and uncertainties due to atmospheric variations and noise in the CCD could be as large as 0.2 mag, the data show a repeating pattern consisting of a linear decline of about 0.5 mag followed by a dip of 0.2 mag and then a sharp rise. The fact that the intervals between all four dips are multiples of 1.932 hr suggests a configuration which repeats at the orbital period. In fact, the mean light curve (Fig. 4*d*), obtained by normalizing each night to a common magnitude and phasing into 20 bins on the 1.932 hr period, shows a quasi-sinusoidal modulation at that period, quite unlike the 2*f* *I*-band ellipsoidal variation seen in the low state (RS[3]). (Unfortunately, the lack of an orbital ephemeris that extends over more than a couple of weeks does not allow us to phase the photometry to the orbital ephemeris.) The behavior in Figure 4*d* perhaps best resembles that of EF Eri and AM Her, in which one accreting pole is always in view, rather than VV Pup or ST LMi, where the primary pole rotates behind the limb of the white dwarf for a significant fraction of the cycle (Cropper 1990).

Our single high-state optical spectrum, shown as Figure 5, exhibits strong, broad (FWZI $\sim$ 58 Å) lines of H and He, with He II λ4686 being most prominent. In all respects (other than the lack of continuum polarization), these data closely resemble the high-state spectra of a generic AM Her in portraying primarily the accretion stream. The optical continuum can be approximately described by $F_\lambda \propto \lambda^{-2.0}$ for $\lambda = 4300$–5100 Å, and likely includes a substantial contribution from gaseous processes in the column.

4.3. *Emission Components in the Low State*

Comparison of the optical spectra in Figure 5 (high state) and Figure 2 (low state) as well as inspection of Table 3 reveals the dramatic spectral changes which occur in the transition of AR UMa between activity states. With the drop in brightness, the lines (especially He II λ4686) decrease

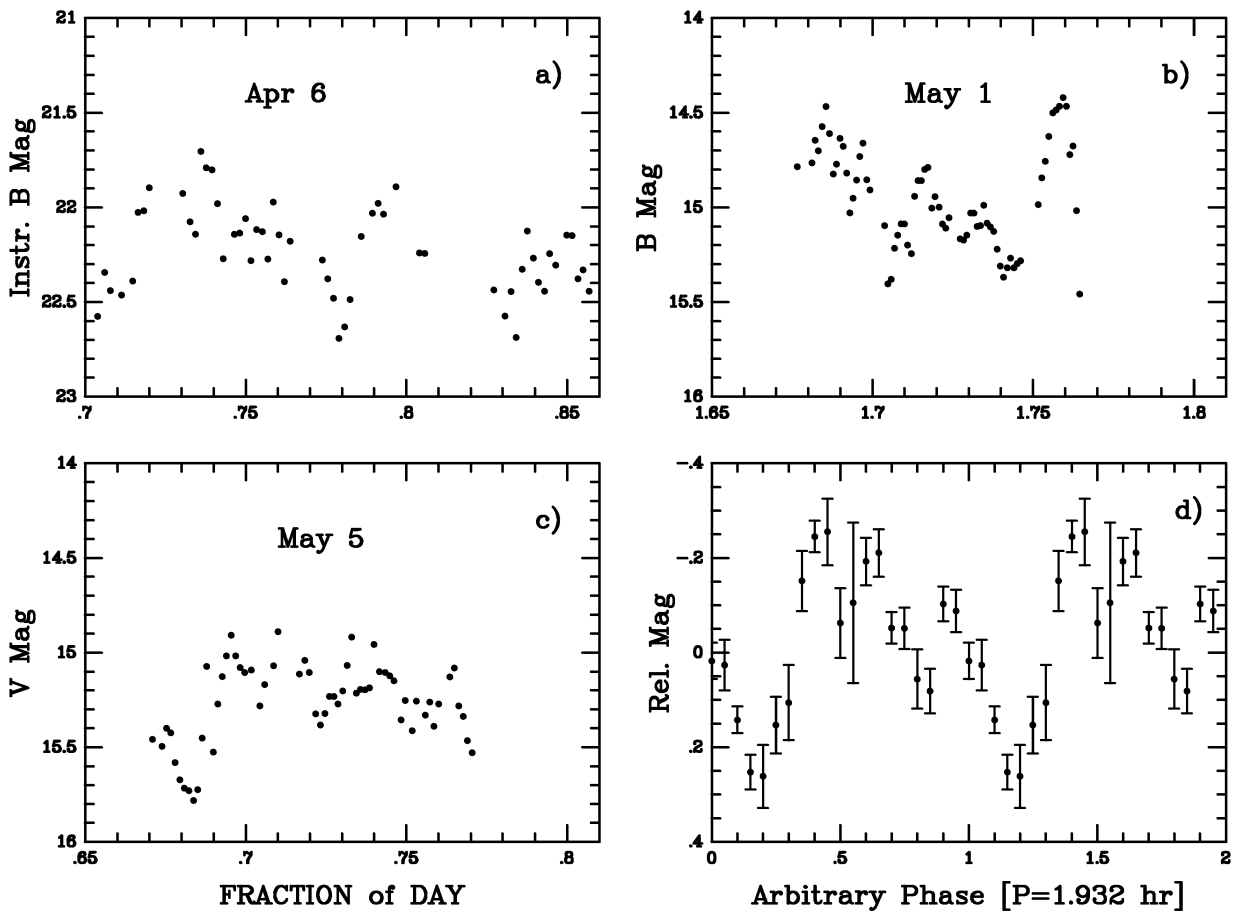

FIG. 4.—(*a*)–(*c*): Three nights of photometry obtained with CCDs on the 1.5 m telescope of OAN. The plots have been made with similar horizontal and vertical scales so the individual nights can be compared. Magnitude scales and errors for each night are discussed in the text. (*d*): Four nights of photometry normalized, folded on a period of 1.932 hr, and summed into 20 bins. The error bars represent the dispersion of values within each bin.

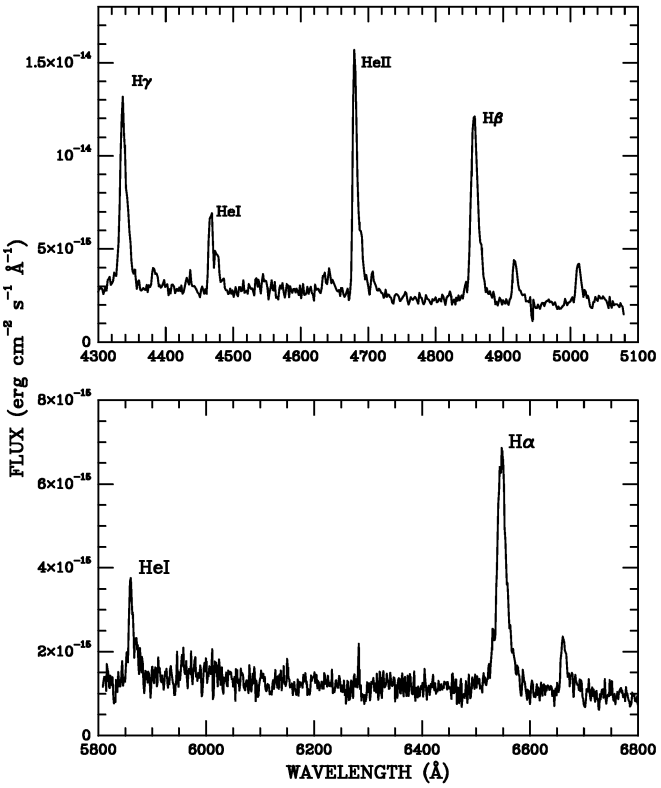

FIG. 5.—High-state optical spectrum obtained with the APO double spectrograph on the same day as the high-state *IUE* spectrum shown in Fig. 3.

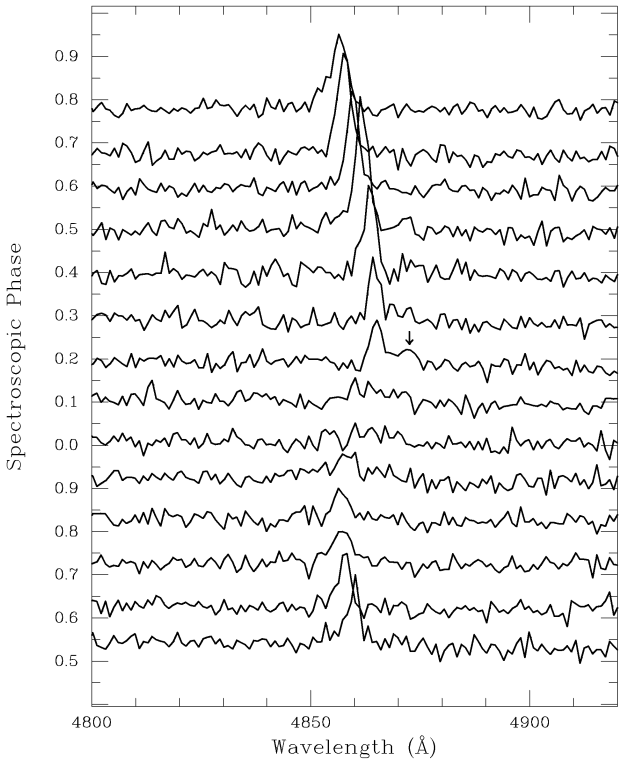

FIG. 6.—Sequence of low-state Hβ profiles measured at high resolution on 1996 January 14. Orbital phases are labeled, with $\phi = 0$ corresponding to positive zero-crossing of the narrow-component radial velocity curve. The "high-velocity" component is indicated at one phase by an arrow.

in intensity and narrow to a FWZI ~ 11 Å. The start of a low state in 1995 November prevented kinematic study of the accretion stream and column but did enable a radial velocity analysis of the narrow emission-line component. As we found in § 4.1, this feature arises from the same location as the narrow-line component in other AM Her systems: the irradiated face of the secondary star.

The strongest feature in the 16 high-resolution spectra from 1996 January 14 is Hβ. Using IRAF routines under SPLOT, the centroid wavelength and total flux of the line were measured. In some of the sequence shown in Figure 6, a separate high-velocity component appeared to be present (indicated for one phase in the figure); however, it could not be followed throughout the orbit, so its phasing is not clear. The velocities of the main component were fitted to a sinusoid with the period fixed at 1.932 hr, yielding parameters as listed in Table 5. Phase 0 was taken to be the crossing from blue to red (corresponding to inferior conjunction of the secondary star) and measured as HJD 2,450,096.9085 ± 0.0015. With this solution, the velocities were phased and are shown together with the measured

TABLE 5

EMISSION-LINE RADIAL VELOCITY SOLUTIONS

Line	γ (km s^{-1})	K (km s^{-1})	ϕ_0[a]
Hβ narrow	−24 ± 12	241 ± 16	0.0
He II λ4686.....	47 ± 19	246 ± 20	−0.05 ± 0.04

[a] $\phi = 0$ is defined as the positive zero-crossing of the Hβ radial velocity curve, which occurs at HJD 2,450,096.9085 ± 0.0015.

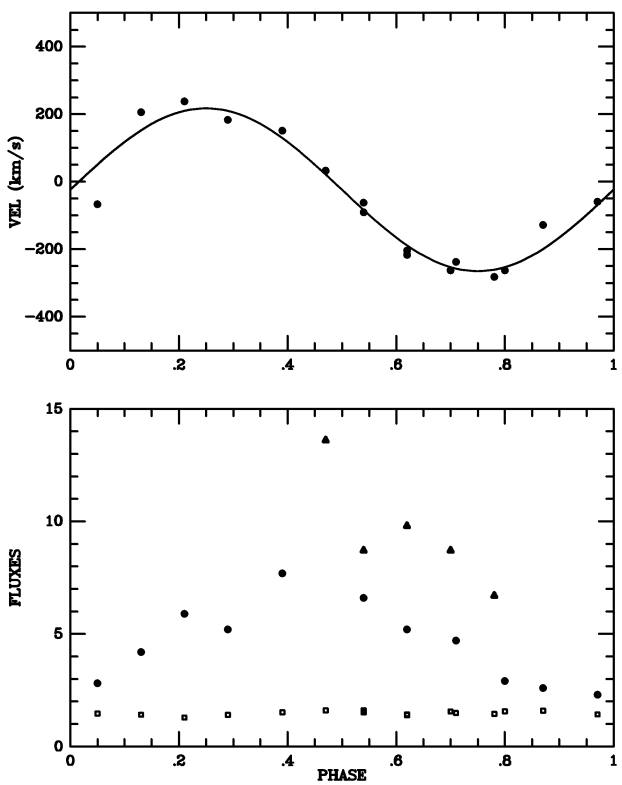

FIG. 7.—*Top:* radial velocity of the main component of Hβ on 1996 January 14 (*filled circles*) compared with the best-fit sinusoid solution (*solid line*). *Bottom:* Hβ line fluxes (*filled circles* and *triangles*) in units of 10^{-15} ergs cm^{-2} s^{-1} and continuum flux near Hβ in units of 10^{-15} ergs cm^{-2} s^{-1} Å^{-1} (*squares*). Triangles indicate the second cycle of coverage.

fluxes in Figure 7. The large increase in line flux (but not the blue continuum) near $\phi = 0.5$ is consistent with an origin of the narrow component on the irradiated secondary. The region of phase overlap suggests that the line flux can undergo large fluctuations from cycle to cycle, with no change in velocity.

With the phase registration adopted above, a Doppler tomogram could be constructed for Hβ. Using a Fourier-filtered back-projection method developed by Horne (1991), the tomogram yields the entire velocity distribution of emitting regions by combining the line profile information from all binary phases. Figure 8 shows the result for AR UMa. The spectra, normalized to a common continuum level and displayed as a trailed gray-scale image in velocity and phase, are shown on the left (the blank line corresponds to the elimination of the spectra near $\phi = 0$ where the lines were very weak). The resulting tomogram is shown on the right, with the usual coordinate system where the secondary is located along the $+V_y$ axis and the white dwarf is along the $-V_y$ axis. The tomogram was also summed along the line of sight at each phase to produce a "forward-projected" trailed spectrum to indicate the reliability of the map. The primary emission region is evident as a compact zone close to the expected location of the secondary. There is some evidence for motion toward the white dwarf (possibly material leaving the secondary in a stream), but the high-velocity component was neither sufficiently strong nor persistent to show up in the tomogram. The bulk of the low-state line emission originates from the secondary, which must remain irradiated even though the accretion rate is greatly reduced.

Further evidence for irradiation comes from the *I*-band photometry during low states. Light curves from 1992 June and 1993 May were presented by RS[3], who pointed out $\sim$0.2 mag ellipsoidal variations from the M star. However, they did not elaborate on the fact that the 1993 variation shows a slightly larger amplitude and $\sim$0.04 mag difference between the minima at at $\phi = 0$ and 0.5. Although an asymmetric light curve can be produced by ellipsoidal effects alone (Bochkarev, Karitskaya, & Shakura 1979), our radial velocities and line strengths imply that the secondary is the source of additional emission seen at phase 0.5. Calculations of the effect of an irradiated secondary on the light curve of U Gem (Berriman et al. 1983) show that a decrease of 0.1 mag in the phase 0.5 amplitude and an increase in the phase 0.0 amplitude occur for an irradiating luminosity near 0.2 $L_\odot$. With a 4.2 hr period, the secondary in U Gem is larger and of earlier type than AR UMa, so a lower irradiating luminosity would be required to achieve the same effects in AR UMa.

We attribute the source of irradiation, which persists well into a low-activity state, to be the heated accretion region of the white dwarf surrounding the magnetic pole. Our *I*-band light curve from 1996 February (Fig. 9, obtained $\sim$3.5 months into a low state), exhibits ellipsoidal variations with a full modulation amplitude of 0.26 mag and difference of $\sim$0.08 mag between primary and secondary mimina. By 1996 March, modulations in the red continuum amounted to 0.08 mag peak-to-peak and an asymmetry between the minima of $\sim$0.02 mag. Although the $\lambda\lambda$6600–7450 region used for the latter measurement is roughly an *R* band, the suggested timescale is consistent with the decline in emission-line strength over the 1995 November–1996 March period depicted in Figure 2. We infer that the cooling timescale of the heated white dwarf is at least a few months (but less than a year) and that accretion essentially turns off during low states. This is unlike most other AM Her systems, which continue to produce X-rays at low states (Cropper 1990). A photometric monitoring campaign throughout a low state would be informative in quantifying this behavior.

The low-state continuum flux near Hβ (Fig. 7) remains constant to within 10% throughout the orbit, displaying neither the $\Delta B \sim 1$ mag changes evident in the high state

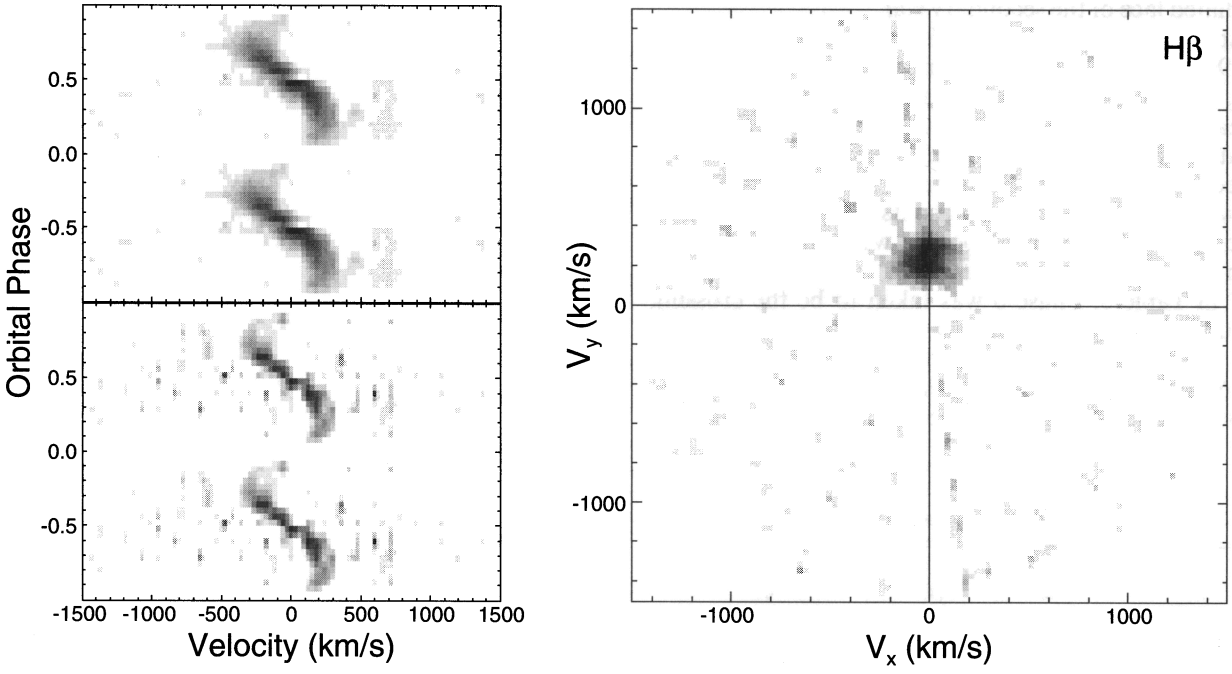

FIG. 8.—Doppler tomogram of the 14 January 1996 spectra. Spectra on the left compare the normalized gray-scale image of the stacked data on the top and the forward-projected spectra obtained from the tomogram on the bottom. The tomogram itself is depicted on the right.

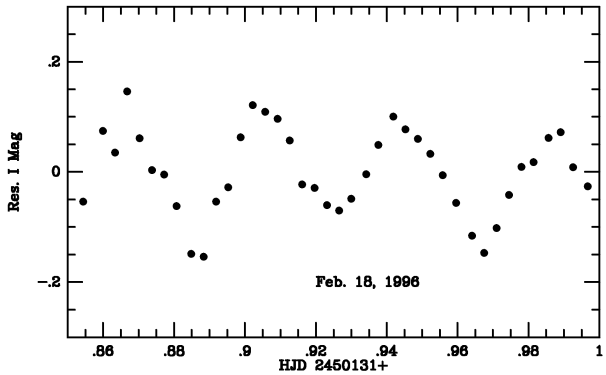

FIG. 9.—Ellipsoidal variations in the *I*-band light curve of AR UMa, obtained approximately 3.5 months into the 1995–1996 low state. Note the different depths of successive minima, indicating the effects of irradiation of the secondary star.

nor the ellipsoidal variations present at *I*. With a spectral shape approximated by $F_\lambda \propto \lambda^{-3.8}$ between 4100 and 5200 Å, the continuum is much bluer than what is measured in the high state and suggests the tail of a hot source which peaks in the UV. Since the source does not change as a function of orbital phase and does not vary with the emission lines, it cannot be ascribed to the irradiated secondary. The logical choice is the white dwarf. To test this conjecture, we combined one of the optical spectra with very weak line emission ($\phi = 0.97$) with the low-state *IUE* spectrum and performed fits to Hubeny (1988) white dwarf models, using solar composition, a gravity fixed at $\log g = 8$, and trying a range of temperatures from 13,000 to 45,000 K. No single-component model was acceptable. A reasonable fit could be obtained for a two-component model, with ~98% of the projected area emitting as a source with $T_{\rm eff} \sim 15{,}000$ K and the remainder by a "spot" with $T_{\rm eff} \sim 35{,}000$ K. The normalization of the fit to the observed flux results in a size for the low-temperature source of $\sim 8 \times 10^8$ cm, which is roughly the radius of a 0.6 $M_\odot$ white dwarf. Since the actual opacities in a stellar atmosphere at 230 MG are unknown, this fit cannot be given much weight, yet the results at face value imply that the hot spot on the white dwarf may be smaller than that found from studies of other magnetic variables (Stockman & Schmidt 1996; Gänsicke, Beuermann, & de Martino 1995; Silber et al. 1996).

5. ACCRETION IN A HIGH-FIELD SYSTEM

A topic of lively discussion in recent years has been the "excess" of soft X-rays observed from several AM Her systems, in the sense that the photon flux of the ~30 eV blackbody exceeds what would be expected for photospheric reprocessing of bremsstrahlung and cyclotron emission from the accretion shock (e.g., Lamb & Masters 1979). The situation was highlighted by the discovery of AM Her itself (and later other systems) in a "reversed" X-ray state, in which the hard and soft components are anticorrelated in strength (Heise et al. 1985). Though several mechanisms have been explored as possible explanations of the problem, a consensus has developed around the idea of inhomogeneities in the accretion stream (Kuijpers & Pringle 1982; Frank, King, & Lasota 1988). Clumps that are overdense by factors of ~10–1000 are stretched into filaments and can penetrate deeply enough into the white dwarf atmosphere for the kinetic energy to be thermalized in a "buried" shock (e.g., Stockman 1988). For AR UMa, hard X-ray information is completely lacking and X-ray observations of any type are sparse. However, the enormous high-state IPC count rate plus rather typical optical brightness suggests a ratio $L_{\rm sx}/L_{\rm opt}$ which may be as much as an order of magnitude greater than a typical AM Her. AR UMa would appear to represent an extreme case of a soft X-ray excess.

If so, the system would strengthen and extend the correlation between soft X-ray excess and magnetic field strength (more specifically, coupling radius, r_c) found by Ramsay et al. (1994). Although Ramsay et al. did not identify a mechanism underlying the relationship, Beuermann & Woelk (1995) discuss the effects which enhanced cyclotron cooling have in reducing the standoff height and eventually burying the shock. While the details of the threading region are far from clear, we note here that the survival of a dense blob against stream instabilities must depend in part on the time available for threading by the field. Once past the L1 point, the gas is very nearly in freefall; thus, the chances for complete threading of a density clump must be increased for systems where coupling occurs further upstream. Our parameters for AR UMa and stream characteristics from Lubow & Shu (1975) imply that the ratio of magnetic to thermal energy density is approximately 10:1 *at the L1 point*. In this binary, even the atmosphere of the secondary star will be threaded, and emerging blobs might well survive as high-density filaments all the way to the white dwarf surface. Note also that, for the field configuration we have presented, dipolar field lines intercepting L1 cannot also lie entirely within the primary star's Roche lobe (see also Ferrario, Wickramasinghe, & Tuohy 1989). Thus, the magnetic field will tend to create a stagnation region in the vicinity of the Roche tip. With feedback provided by radiative heating from the accretion shock, an oscillatory behavior might be set up which could play a significant role in the decidedly episodic nature of mass-transfer in this binary.

6. DISCOVERY AND EVOLUTIONARY CONSIDERATIONS

Despite the fact that isolated magnetic white dwarfs and magnetic CVs are known in roughly equal numbers (about four dozen each), several single magnetic stars have been found with $B \gtrsim 500$ MG (e.g., Schmidt & Smith 1995), while the maximum field strength in a white dwarf binary has been ~70 MG. Proposed remedies to this long-standing puzzle have included both evolutionary as well as identification considerations.

Liebert & Stockman (1985; see also King 1985; Schmidt, Stockman, & Grandi 1986a) proposed that high-field synchronized systems would suffer accelerated period evolution by "cooperative" magnetic braking of the two stars. Such binaries would lead short but brilliant lives, rendering them rare and perhaps unique in appearance. With this in mind, Stockman et al. (1992) surveyed a few supposed neutron star X-ray binaries for circular polarization, with null results.

In the standard model for CV evolution, enhanced braking would also widen the 2–3 hr period gap (Hameury et al. 1987). In fact, the gap is narrower or even nonexistent for the magnetic systems (Kolb & de Kool 1993). Thus, Wickramasinghe & Wu (1994; see also Li, Wu, & Wickramasinghe 1994) have proposed quite the opposite scenario: in the synchronized magnetic systems, a significant fraction of the secondary's field lines close on the white

dwarf. This leads to *decreased* braking efficiency and lower accretion rates. The period gap is narrowed or closed altogether for magnetic objects, and braking is so inefficient for $B \gtrsim 70$ MG that long-period systems take an inordinate amount of time to reach contact under gravitational radiation alone.

Given the number of magnetic CVs now known, our discovery of one high-field AM Her does not fundamentally alter the situation. Indeed, at $P < 2$ hr, magnetic braking would have ceased even under normal (nonmagnetic) CV evolution, so AR UMa does not directly test the idea that the white-dwarf field inhibits the mechanism. However, in the context of that theory, the mere existence of the binary requires that at least some magnetic CVs emerge from the common envelope at short orbital periods $P \lesssim 8$ hr. The high luminosity of AR UMa (dominated by X-rays) would instead seem to support enhanced angular momentum loss. However, this too must be viewed with caution, since models of the secondary's response to the resumption of mass transfer immediately below the period gap show that the accretion rate can be temporarily doubled over stable rates thereafter, even when angular momentum loss is restricted to that from gravitational radiation (McDermott & Taam 1989).

The fact that AR UMa was detected in circular polarization only after lapsing into a low-accretion state raises the possibility that selection effects play a role in the apparent lack of high-field systems. Stockman et al. (1992) considered this question in the context of an extensive polarimetric survey of known CVs. They noted that objects with $B > 100$ MG would still lack a diluting accretion disk and exhibit X-ray and emission-line spectra very similar to known AM Her binaries and hence would not be overlooked in CV surveys. These traits are borne out by AR UMa. Not anticipated, however, was the strikingly bimodal activity cycle, which presumably accounts for the absence of AR UMa in other all-sky X-ray surveys. The failure to polarimetrically detect the system in the high state is apparently due to high cyclotron opacity near the fundamental coupled with an unfavorable viewing geometry (for circular polarization). Remarkably, Stockman et al. predicted that even if the cyclotron light were absent or unpolarized, photospheric emission from a high-field primary would result in a polarization of $V/I = 2\%$–5% when the system entered a low-accretion state. This describes precisely the situation surrounding the discovery of magnetism in AR UMa. Recalling the lesson learned from the initial field strength measurement of AM Her itself (Schmidt et al. 1981), we suggest that future polarimetric searches for high-field systems should specifically target soft X-ray sources during faint states.

7. SUMMARY

AR UMa is an important new example of a magnetic cataclysmic variable. An extremely luminous soft X-ray source which is only weakly polarized when accreting, the system is prone to abrupt and protracted changes in activity state. Mass transfer appears to cease altogether when the binary lapses into a low state. At this time, the stellar components can be discerned: a phase-locked magnetic white dwarf primary with the strongest field yet identified in a mass-transfer system plus a low-mass M-type companion in a 1.932 hr orbit. The extreme field is quantified at $B \sim 230$ MG through our identification of a Zeeman-split absorption component of Lyα in the UV, but the sizable low-state continuum circular polarization plus a hot optical continuum component containing a number of unidentified, strongly polarized absorption features substantiate the conclusion.

The strong magnetic field clearly plays a role in the accretion physics of the binary. Dense blobs in the stream are likely fully threaded by the field from the time they leave the L1 point. The resulting accretion filaments manage to avoid a shock above the white dwarf, to have their kinetic energy deposited below the photosphere. This accounts in part for the lack of polarized cyclotron emission in the optical and creates an extreme example of an object with a soft X-ray "excess." In the first few months following the end of a high state, reprocessing by the irradiated secondary is seen to decline as the heated accretion pole of the white dwarf cools. The added pressure provided by the magnetic field near the secondary's Roche tip may create an instability in the gas flow through the L1 point, thereby contributing to the unusually episodic behavior pattern of this binary.

We thank Keith Horne for providing his software for the Doppler tomography routines. Jim Liebert, Fulvio Melia, and Pete Stockman shared interesting ideas on high-field magnetic accretion binaries. This work was supported by NASA grants NAGW-3158, NAG5-1927, NAG5-2114, and NAG5-1630, by NSF grants AST 92-17911 to P. S. and AST 91-14087 to G. D. S., and by DGAPA-UNAM project IN-109195 to G. T.

REFERENCES

Berriman, G., Beattie, D. H., Gatley, I., Lee, T. J., Mochnacki, S. W., & Szkody, P. 1983, MNRAS, 204, 1105
Beuermann, K., & Woelk, U. 1996, in Proc. IAU Colloq. 158, Cataclysmic Variables and Related Objects, ed. A. Evans & J. H. Wood (Dordrecht: Kluwer), 199
Bochkarov, N. G., Karitskaya, E. A., & Shakura, N. I. 1979, Soviet Astron., 23, 8
Bonnet-Bidaud, J. M., & Mouchet, M. 1987, A&A, 188, 89
Campbell, C. G. 1983, MNRAS, 205, 1031
———. 1989, MNRAS, 236, 475
———. 1990, MNRAS, 244, 367
Cropper, M. 1988, MNRAS, 231, 597
———. 1990, Space Sci. Rev., 54, 195
de Martino, D. 1995, in ASP Conf. Ser. 85, Cape Workshop on Magnetic Cataclysmic Variables, ed. D. A. H. Buckley & B. Warner (San Francisco: ASP), 238
Ferrario, L., Wickramasinghe, D. T., Bailey, J. A., Buckley, D. A. H., & Hough, J. H. 1994, MNRAS, 268, 128
Ferrario, L., Wickramasinghe, D.T., & Tuohy, I. R. 1989, ApJ, 341, 327
Frank, J., King, A. R., & Lasota, J.-P. 1988, A&A, 193, 113
Gänsicke, B. T., Beuermann, K., & de Martino, D. 1995, A&A 303, 127
Glenn, J., Liebert, J., & Schmidt, G. D. 1994, PASP, 106, 722
Hameury, J. M., King, A. R., Lasota, J.-P., & Ritter, H. 1987, ApJ, 316, 275
Heise, J., Brinkman, A. C., Gronenschild, E., Watson, M., King, A. R., Stella, L., & Kieboom, K. 1985, A&A, 148, L14
Honeycutt, R. K., Robertson, J. W., & Turner, G. W. 1996, private communication
Horne, K. 1991, in Fundamental Properties of Cataclysmic Variable Stars, ed. A. W. Shafter (San Diego: SDSU), 23
Hubeny, I. 1988, Comput. Phys. Comm. 52, 103
Joss, P. C., Katz, J. I., & Rappaport, S. A. 1979, ApJ, 230, 176
Katz, J. I. 1989, MNRAS, 239, 751
Kemic, S. B. 1974, JILA Rep. 113, Univ. Colorado
King, A. R. 1985, MNRAS, 217, 23P
King, A. R., Frank, J., & Whitehurst, R. 1990, MNRAS, 244, 731
Kolb, U., & de Kool, M. 1993, in ASP Conf. Ser. 56, Interacting Binary Stars, ed. A. W. Shafter (San Francisco: ASP), 338
Kuijpers, J., & Pringle, J. E. 1982, A&A, 114, L4
Lamb, D. Q. 1985, in Proc. 7th North American Workshop on Cataclysmic Variables and Low-Mass X-Ray Binaries, ed. D. Q. Lamb & J. Patterson (Dordrect: Reidel), 179

Lamb, D. Q., & Masters, A. R. 1979, ApJ, 234, L117
Lamb, D. Q., & Melia, F. 1988, in Polarized Radiation of Circumstellar Origin, ed. G. V. Coyne, A. M. Magalhaes, A. F. J. Moffat, R. E. Schulte-Ladbeck, S. Tapia, & D. T. Wickramasinghe (Vatican City: Vatican Observatory), 45
Latter, W. B., Schmidt, G. D., & Green, R. F. 1987, ApJ, 320, 308
Li, J., Wu, K., & Wickramasinghe, D. T., 1994, MNRAS, 268, 61
Liebert, J., Bergeron, P., Schmidt, G. D., & Saffer, R. A. 1993, ApJ, 418, 426
Liebert, J., & Stockman, H. S. 1985, in Proc. 7th North American Workshop on Cataclysmic Variables and Low-Mass X-Ray Binaries, ed. D. Q. Lamb & J. Patterson (Dordrect: Reidel), 151
Lubow, S. H., & Shu, F. H. 1975, ApJ, 198, 383
McDermott, P. N., & Taam, R. E. 1989, ApJ, 342, 1019
Norton, A. J., & Watson, M. G. 1989, MNRAS, 237, 715
Ramsay, G., Mason, K. O., Cropper, M., Watson, M. G., & Clayton, K. L. 1994, MNRAS, 270, 692
Remillard, R. A., Schachter, J. F., Silber, A. D., & Slane, P. 1994, ApJ, 426, 288 (RS^3)
Ruder, H., Wunner, G., Herold, H., & Geyer, F. 1994, Atoms in Strong Magnetic Fields (Berlin: Springer)
Schmidt, G. D., Allen, R., Smith, P. S., & Liebert, J. 1996, ApJ, 463, 320
Schmidt, G. D., Latter, W. B., & Foltz, C. B. 1990, ApJ, 350, 758
Schmidt, G. D., & Smith, P. S. 1995, ApJ, 448, 305
Schmidt, G. D., Stockman, H. S., & Grandi, S. A. 1986a, ApJ, 300, 804
Schmidt, G. D., Stockman, H. S., & Margon, B. 1981, ApJ, 243, L157
Schmidt, G. D., West, S. C., Liebert, J., Green, R. F., & Stockman, H. S. 1986b, ApJ, 309, 218
Schwope, A. D., Beuermann, K., Jordan, S., & Thomas, H.-C. 1993, A&A, 278, 487
Schwope, A. D., Thomas, H.-C., Beuermann, K., Burwitz, V., Jordan, S., & Haefner, R. 1995, A&A, 293, 764
Silber, A. D., Raymond, J. C., Mason, P. A., Andronov, I. L., Borisov, N., & Shakhovskoy, N. M. 1996, ApJ, 460, 939
Stockman, H. S. 1988, in Polarized Radiation of Circumstellar Origin, ed. G. V. Coyne, A. M. Magalhaes, A. F. J. Moffat, R. E. Schulte-Ladbeck, S. Tapia, & D. T. Wickramasinghe (Vatican City: Vatican Observatory), 237
Stockman, H. S., & Schmidt, G. D. 1996, ApJ, 468, 883
Stockman, H. S., Schmidt, G. D., Berriman, G., Liebert, J., Moore, R. L., & Wickramasinghe, D. T. 1992, ApJ, 401, 628
Thurner, G., Körbel, H., Braun, M., Herold, H., Ruder, H., & Wunner, G. 1993, J. Phys. B, 26, 4719
Wickramasinghe, D. T., Visvanathan, N., & Tuohy, I. R. 1984, ApJ, 286, 328
Wickramasinghe, D. T., & Wu, K. 1991, MNRAS, 253, 11P
———. 1994, MNRAS, 266, L1
Wu, K., & Wickramasinghe, D. T. 1993, MNRAS, 260, 141